

UC Davis

UC Davis Previously Published Works

Title

Activation of Tm-22 resistance is mediated by a conserved cysteine essential for tobacco mosaic virus movement.

Permalink

<https://escholarship.org/uc/item/0xz8n8v6>

Journal

Molecular Plant Pathology, 24(8)

Authors

Hak, Hagit
Raanan, Hagai
Schwarz, Shahar
[et al.](#)

Publication Date



2023-08-01

DOI

10.1111/mpp.13318

Peer reviewed

Activation of *Tm-2²* resistance is mediated by a conserved cysteine essential for tobacco mosaic virus movement

Hagit Hak¹ | Hagai Raanan^{1,2} | Shahar Schwarz¹ | Yifat Sherman^{1,3} |
Savithamma P. Dinesh-Kumar⁴  | Ziv Spiegelman¹ 

¹Department of Plant Pathology and Weed Research, Agricultural Research Organization, The Volcani Institute, Rishon LeZion, Israel

²Gilat Research Center, Agricultural Research Organization, Negev, Israel

³The Robert H. Smith Faculty of Agriculture, Food and Environment, The Hebrew University of Jerusalem, Rehovot, Israel

⁴Department of Plant Biology and Genome Center, College of Biological Sciences, University of California, Davis, California, USA

Correspondence

Ziv Spiegelman, Department of Plant Pathology and Weed Research, Agricultural Research Organization, The Volcani Institute, 68 HaMaccabim Road, P.O.B. 15159, Rishon LeZion 7505101, Israel.

Email: ziv.spi@volcani.agri.gov.il

Funding information

Ministry of Agriculture and Rural Development, Grant/Award Number: 20-02-0130; United States - Israel Binational Agricultural Research and Development Fund, Grant/Award Number: IS-5386-21

Abstract

The tomato *Tm-2²* gene was considered to be one of the most durable resistance genes in agriculture, protecting against viruses of the *Tobamovirus* genus, such as tomato mosaic virus (ToMV) and tobacco mosaic virus (TMV). However, an emerging tobamovirus, tomato brown rugose fruit virus (ToBRFV), has overcome *Tm-2²*, damaging tomato production worldwide. *Tm-2²* encodes a nucleotide-binding leucine-rich repeat (NLR) class immune receptor that recognizes its effector, the tobamovirus movement protein (MP). Previously, we found that ToBRFV MP (MP^{ToBRFV}) enabled the virus to overcome *Tm-2²*-mediated resistance. Yet, it was unknown how *Tm-2²* remained durable against other tobamoviruses, such as TMV and ToMV, for over 60 years. Here, we show that a conserved cysteine (C68) in the MP of TMV (MP^{TMV}) plays a dual role in *Tm-2²* activation and viral movement. Substitution of MP^{ToBRFV} amino acid H67 with the corresponding amino acid in MP^{TMV} (C68) activated *Tm-2²*-mediated resistance. However, replacement of C68 in TMV and ToMV disabled the infectivity of both viruses. Phylogenetic and structural prediction analysis revealed that C68 is conserved among all Solanaceae-infecting tobamoviruses except ToBRFV and localizes to a predicted jelly-roll fold common to various MPs. Cell-to-cell and subcellular movement analysis showed that C68 is required for the movement of TMV by regulating the MP interaction with the endoplasmic reticulum and targeting it to plasmodesmata. The dual role of C68 in viral movement and *Tm-2²* immune activation could explain how TMV was unable to overcome this resistance for such a long period.

KEYWORDS

movement protein, plasmodesmata, *Tm-2²*, TMV, *Tobamovirus*, ToBRFV

1 | INTRODUCTION

Plant viruses cause diseases that severely restrict crop production. Some of the most harmful plant viruses are members of the *Tobamovirus* genus, such as tomato mosaic virus (ToMV) and tobacco mosaic virus (TMV). Viral symptoms include severe plant yellowing and

stunting, and reductions in yield and fruit quality, and these viruses are highly transmissible by mechanical contact (Broadbent, 1976). The tobamovirus genome consists of a single-stranded, positive-sense RNA of about 6.4 kb that encodes two subunits of an RNA-dependent RNA polymerase (RdRp), a movement protein (MP) and a coat protein (CP) (Goelet et al., 1982). Successful infection depends on the MP, which

This is an open access article under the terms of the [Creative Commons Attribution-NonCommercial-NoDerivs](https://creativecommons.org/licenses/by-nc-nd/4.0/) License, which permits use and distribution in any medium, provided the original work is properly cited, the use is non-commercial and no modifications or adaptations are made.

© 2023 The Authors. *Molecular Plant Pathology* published by British Society for Plant Pathology and John Wiley & Sons Ltd.

enables the virus to move from cell to cell (Navarro et al., 2019). MP binds to the viral RNA, targets it to plasmodesmata (PD), membrane-lined channels interconnecting adjacent cells, and increases the PD size exclusion limit in a process termed gating (Reagan & Burch-Smith, 2020). These processes depend on various MP attributes, including its specific subcellular targeting, interaction with cellular factors (e.g., endoplasmic reticulum [ER] and microtubules), and the binding of multiple host proteins (Pitzalis et al., 2018).

Dominant resistance (*R*) genes in plants are pivotal factors for the control of plant pathogens in agriculture. Most *R* genes encode the nucleotide-binding leucine-rich repeat (NLR) class of immune receptors that confer resistance by recognizing specific pathogen-derived molecules named effectors (Adachi et al., 2019; Jones & Dangl, 2006). On effector recognition, NLRs oligomerize into a structure named the resistosome to form a calcium-permeable plasma membrane channel (Bi et al., 2021; Martin et al., 2020; Wang et al., 2019). The formed calcium influx then induces programmed cell death of the infected plant tissue that limits pathogen infection in a process termed the hypersensitive response (HR) (Meier et al., 2019). The tomato *Tm-2* gene encodes an NLR that confers protection against viruses of the *Tobamovirus* genus, including TMV and ToMV. *Tm-2* recognizes and associates with the viral MP, the effector, to trigger the resistance response against tobamoviruses (Chen et al., 2017; Weber et al., 1993). This recognition results in the self-association of *Tm-2*, which activates HR-mediated immunity against the virus (Wang et al., 2020).

Until recently, *Tm-2* was considered one of the most durable *R* genes in agriculture (Hall, 1980). However, a newly emerged tobamovirus named tomato brown rugose fruit virus (ToBRFV) has overcome all tobamovirus resistance genes, including *Tm-2*, and caused substantial damage to the global tomato industry (Luria et al., 2017; Zhang et al., 2022). Recently, we found that the MP of ToBRFV (MP^{ToBRFV}) is the viral factor that enables ToBRFV to overcome *Tm-2* resistance (Hak & Spiegelman, 2021). Expression of MP^{ToBRFV} failed to trigger *Tm-2*-mediated HR and substitution of the original MP sequence of the nonresistance-breaking virus ToMV with MP^{ToBRFV} enabled the recombinant virus to overcome *Tm-2* resistance in tomato. Another recent study mapped the six amino acids in MP^{ToBRFV} (H67, N125, K129, A134, I147, and I168) required for ToBRFV to overcome *Tm-2*, pinpointing the precise sites that enable evasion of *Tm-2*-mediated resistance (Yan et al., 2021).

Because the MP is crucial for intercellular movement, we hypothesized that mutations that enable the MP to overcome *Tm-2*-mediated resistance may also affect cell-to-cell movement of the virus. Our recent findings indicated that MP^{ToBRFV} cell-to-cell movement was reduced compared to MP of TMV (MP^{TMV}) (Hak & Spiegelman, 2021). The potential trade-off between *Tm-2* immune evasion and viral movement could explain the high durability of *Tm-2* against TMV and ToMV. However, whether such a trade-off exists and the potential mechanism underlying it are currently unknown. Here, we show that the presence of a cysteine residue (C68) conserved among Solanaceae-infecting tobamovirus movement proteins activates *Tm-2* resistance. Our results show that the C68 is required for TMV and ToMV movement by

directing MP movement on the ER and subsequent localization to PD. Interestingly, in MP^{ToBRFV}, the corresponding position is occupied by histidine (H67), but intercellular movement is sustained. The lack of tolerance to mutations in C68 can therefore explain how TMV and ToMV were unable to overcome *Tm-2* for over 60 years.

2 | RESULTS

2.1 | The presence of C68 in the MP triggers *Tm-2* resistance

Transient co-expression of MP^{TMV} with *Tm-2* in *Nicotiana benthamiana* leaves results in the appearance of HR-mediated cell death due to *Tm-2* immune activation (Figure 1a,b; Hak & Spiegelman, 2021). In contrast, co-expression of MP^{ToBRFV} with *Tm-2* resulted in only minor cell death (Figures 1a,b and S1). To determine regions of the MP^{TMV} that activate *Tm-2*, two hybrid MP^{TMV}/MP^{ToBRFV} clones were generated. Fusion of MP^{TMV} amino acids 1 to 50 to MP^{ToBRFV} amino acids 51 to 266 (MP^{ToBRFV} 1-50/MP^{TMV} 217-266) failed to activate *Tm-2* (Figure S1). However, MP^{TMV} amino acids 1 to 110 fused to MP^{ToBRFV} amino acids 110 to 266 (MP^{TMV} 1-110/MP^{ToBRFV} 111-266) triggered the *Tm-2* response (Figure S1). These results suggested that elements within MP^{TMV} amino acids 51-110 are required for the activation of *Tm-2*. Among the MP^{ToBRFV} amino acids required for overcoming *Tm-2*-mediated resistance (Yan et al., 2021), histidine 67 (H67) is the only one that localizes to this region. To test if H67 and the corresponding amino acid in MP^{TMV}, cysteine 68 (C68), are determinants of the *Tm-2* immune response, we used site-directed mutagenesis to introduce reciprocal mutations in MP^{TMV} and MP^{ToBRFV}, thereby changing both amino acids to their identity in the corresponding virus. Indeed, the replacement of MP^{ToBRFV} H67 with cysteine (MP^{ToBRFV} H67C) triggered strong HR cell death when co-expressed with *Tm-2* (Figure 1a,b). When H67 was replaced with another amino acid, serine (MP^{ToBRFV} H67S), it failed to trigger *Tm-2*-mediated HR cell death, suggesting a specific role for cysteine in *Tm-2* activation (Figure 1a,b). On the other hand, replacement of MP^{TMV} C68 with histidine (MP^{TMV} C68H) still triggered HR when co-expressed with *Tm-2* (Figure 1a,b), indicating that MP^{TMV} elements other than C68 are also capable of activating the *Tm-2* response.

2.2 | MP^{TMV} C68 is conserved in sequence and structure

C68 localizes to a region essential for protein folding (Citovsky et al., 1992) and for association with the ER (Peiro et al., 2014), suggesting its putative function in cell-to-cell movement. To determine the conservation of C68, protein sequence alignment of Solanaceae-infecting tobamoviruses was performed (Figures 2a and S2). This analysis revealed that C68 is highly conserved, while H67 is unique to MP^{ToBRFV}, suggesting a role for C68 among Solanaceae-infecting tobamoviruses.

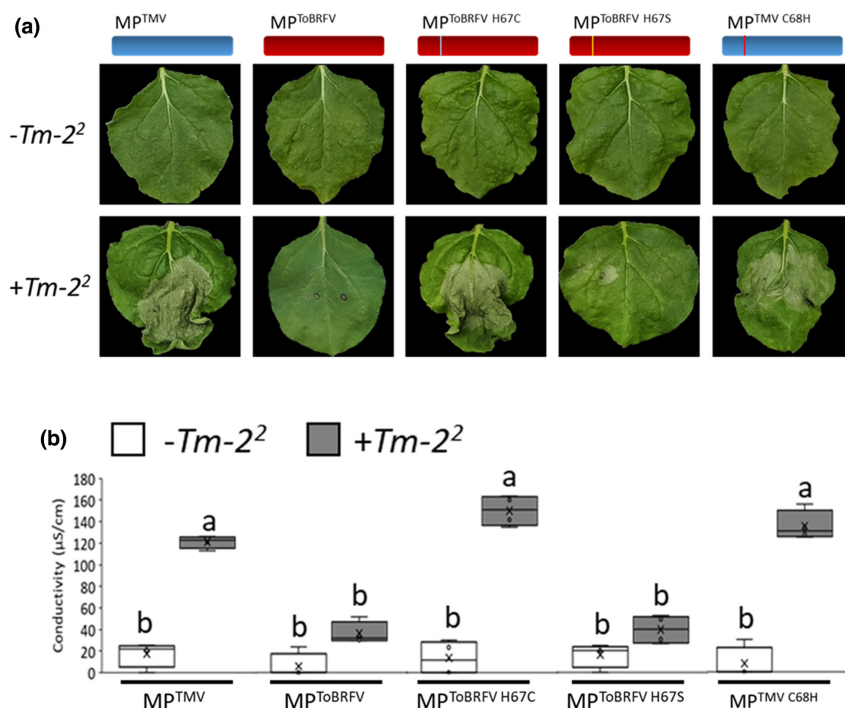


FIGURE 1 *Tm-2* resistance is activated in the presence of movement protein amino acid C68. (a) Images of *Nicotiana benthamiana* leaves transiently expressing MP^{TMV}, MP^{ToBRFV}, MP^{ToBRFV H67C}, MP^{ToBRFV H67S} or MP^{TMV C68H} co-expressed with an empty vector (-*Tm-2*) or with *Tm-2* (+*Tm-2*). Photographs were taken 48 h after infiltration. (b) Electrolyte leakage assay of *N. benthamiana* leaves expressing each construct along with an empty vector (-*Tm-2*) or *Tm-2* (+*Tm-2*). Different letters indicate significance in Tukey's HSD test ($p < 0.05$, $n \geq 5$).

To determine the importance of H67/C68, we performed three-dimensional (3D) protein structural analysis of MP^{TMV} and MP^{ToBRFV}. As there are no existing 3D structures for any tobamovirus MPs, we used the AlphaFold2 modelling platform (Jumper et al., 2021). These analyses provided high-confidence predictions for both proteins, including at the H67/C68 position (Figures 2b,c and S3). Based on this analysis, C68/H67 localized to a jelly-roll fold, typical of various viral proteins (Krupovic et al., 2022), which contains two previously identified membrane interactions motifs (Figure 2b; Peiro et al., 2014). To explore the conservation of this fold, the structure of four other members of the 30K MP superfamily was modelled using AlphaFold2: MP of cauliflower mosaic virus (MP^{CaMV}), MP of cucumber mosaic virus (MP^{CMV}), MP of tomato bushy stunt virus (MP^{TBSV}), and MP of tomato spotted wilt virus (MP^{TSWV}) (Figure 2d). Interestingly, this analysis revealed a putative jelly-roll fold conserved among all these analysed MPs. These results suggest that C68 is localized in an MP region conserved in sequence, structure, and function, and possibly plays a dual role in both activating the *Tm-2* immune response and cell-to-cell movement.

2.3 | C68 is essential for TMV and ToMV infection

The conservation of C68 suggests a role for this amino acid in viral infection. To test the function of C68, the C68H mutation was introduced into a ToMV infectious clone (ToMV^{MP(C68H)-ToMV}) (Hamamoto et al., 1993). Tomato plants homozygous for the ToMV-sensitive *tm-2* allele or the *Tm-2* resistance allele were then inoculated with the mutant viral RNA (Figure 3a). As controls, plants were also inoculated with nonmutant ToMV and a hybrid version of ToMV harbouring MP^{ToBRFV} (ToMV^{MP-ToBRFV}) replacing its original MP (Hak & Spiegelman, 2021). Four plants from each treatment were tested 3 weeks after inoculation for appearance of visual symptoms and presence of viral proteins

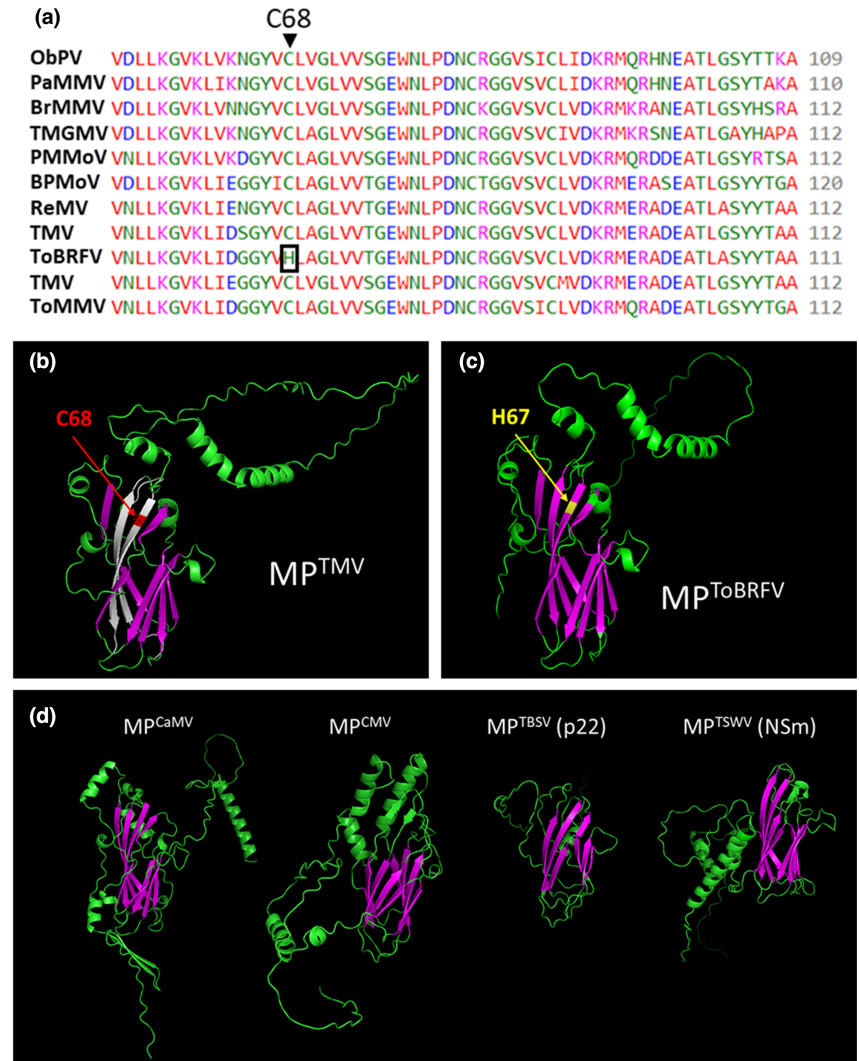
by immunoblot analysis. As expected, ToMV successfully infected *tm-2* plants, but not *Tm-2* plants (Figure 3a,b). Consistent with our previous report (Hak & Spiegelman, 2021), the ToMV^{MP-ToBRFV} also infected both *tm-2* and *Tm-2* plants (Figure 3a,b). However, ToMV^{MP(C68H)-ToMV} could not infect both genotypes (Figure 3a,b).

To explore whether the function of C68 is conserved across tobamoviruses and host species, we generated TMV-GFP recombinant virus clones (Lindbo, 2007) containing the MP^{ToBRFV} (TMV-GFP^{MP-ToBRFV}) or MP (C68H) mutant (TMV-GFP^{MP(C68H)-TMV}) in place of the original TMV MP (Figure 3c). Green fluorescent protein (GFP) fluorescence levels were monitored in systemic leaves (fourth leaf from the apex) using the in vivo imaging system (IVIS) (Figure 3d). TMV-GFP and TMV-GFP^{MP-ToBRFV} systemically infected *N. benthamiana* plants (Figure 3c,d). However, TMV-GFP^{MP(C68H)-TMV} was unable to infect *N. benthamiana* plants (Figure 3c,d). These results establish that the amino acid C68 in MP is essential for the systemic infection of both TMV and ToMV in *N. benthamiana* and tomato, respectively. In addition to C68H, we generated other mutations in MP^{TMV} that match their respective identity in MP^{ToBRFV} (Figure S4). These include deletion of valine 5 ($\Delta V5$) and replacement of asparagine 169 with isoleucine (N169I), which is also required for overcoming *Tm-2* (Yan et al., 2021). Neither mutation disabled TMV-GFP from infecting *N. benthamiana* plants (Figure S4), suggesting a unique role for C68 in TMV cell-to-cell movement and therefore infectivity.

2.4 | Intercellular movement of MP^{TMV} relies on C68

The loss of systemic infection in TMV and ToMV C68H mutants (Figure 3) suggests that C68 is essential for MP function. To determine the effect of C68H on MP cell-to-cell movement, we examined the

FIGURE 2 Conservation of C68 in sequence and structure. (a) Protein sequence alignment of Solanaceae-infecting tobamovirus movement proteins. C68 is highlighted by a black arrow and ToBRFV H67 is highlighted by a black square. (b–d) AlphaFold models of MP^{TMV} (b), MP^{ToBRFV} (c), and four distant members of the 30K movement protein superfamily (MP^{CaMV}, MP^{CMV}, MP^{TBSV}, and MP^{TSWV}) (d). Purple marks the conserved β -barrel fold. The white arrows in (b) show the hydrophobic endoplasmic reticulum association regions previously described by Peiro et al. (2014). The red arrow marks C68 in MP^{TMV} (b) and the yellow arrow marks H67 in MP^{ToBRFV} (c).



TMV-GFP inoculation sites in *N. benthamiana* leaves 5 days after inoculation (Figure 4). At this time point, the virus is already replicating and moving from cell to cell, resulting in round infection foci. The TMV-GFP infection foci size was 1.2 mm² (Figure 4a,d). Consistent with its reduced mobility, the TMV-GFP^{MP-ToBRFV} infection foci size was 0.5 mm² (Figure 4b,d). Strikingly, TMV-GFP^{MP(C68H)-TMV} was able to replicate in the infected cells but could not move out of proximal cells (Figure 4c,d), suggesting that C68 is required for TMV cell-to-cell movement.

To further examine if C68 is required for MP movement, MP open reading frames were fused to a gene encoding yellow fluorescent protein (YFP) and expressed under control of the cauliflower mosaic virus 35S promoter. ER-targeted mCherry (ER-mCherry) was expressed from the same binary plasmid as a nonmobile control marking the original cell of expression. *N. benthamiana* leaves were infiltrated with a low dilution of *Agrobacterium* to express the constructs in distinct epidermal cells as previously described (Hak & Spiegelman, 2021). We observed intercellular movement of both MP^{TMV} and MP^{ToBRFV} (Figure 5a–f,j–k). However, the C68H mutation abolished cell-to-cell movement of MP^{TMV} (Figure 5g–k). Replacement of other MP^{TMV} amino acids with the corresponding MP^{ToBRFV} amino acids required for overcoming *Tm-2*², N135A and

N169I, did not disable intercellular movement of MP^{TMV} (Figure S5), suggesting that C68 plays an important role in controlling the movement function of MP^{TMV}.

2.5 | C68 is required for the localization of MP^{TMV} to the ER and PD

To examine how replacement of C68 resulted in the loss of MP^{TMV} cell-to-cell movement, we analysed the subcellular localization of MP^{TMV} C68H to PD using aniline blue callose staining (Figure 6). Plasmodesmatal localization was calculated as the ratio between the MP-YFP fluorescent signal intensity colocalized with callose at PD and the MP-YFP signal intensity along the plasma membrane (PM) at the cell perimeter (Figure 6a,e). This ratio indicated the level of MP specific localization to PD. MP^{TMV}-YFP showed the highest PD localization (Figure 6a,e). In MP^{ToBRFV}-YFP, plasmodesmatal localization was also evident, but 25% reduced as compared to MP^{TMV} (Figure 6b,e), a result consistent with its reduced cell-to-cell movement. Strikingly, the MP^{TMV(C68H)}-YFP mutant was not distinctly targeted to PD (Figure 6c,e). Instead, this protein localized to

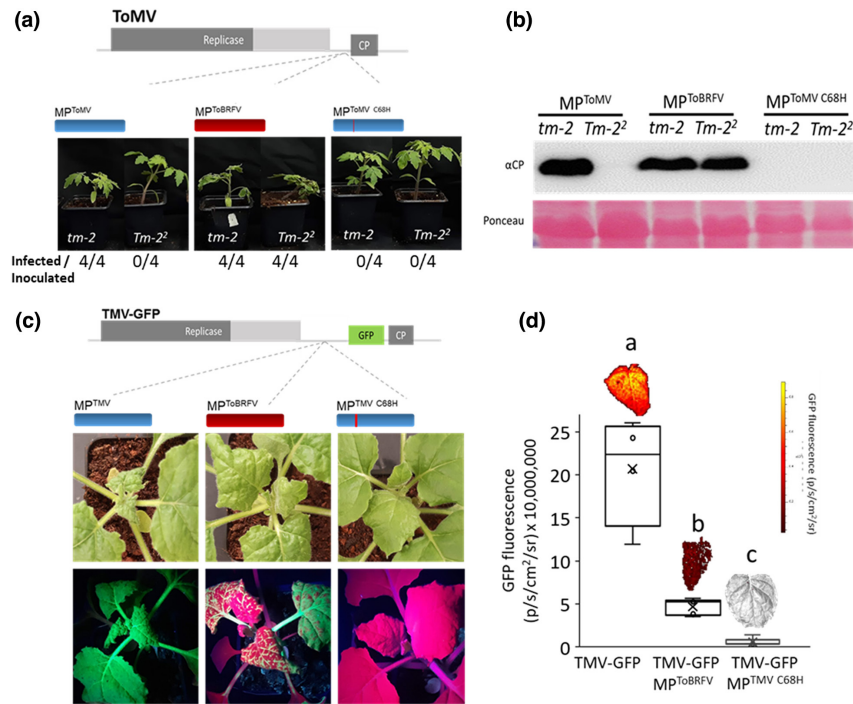


FIGURE 3 Substitution of movement protein (MP) amino acid C68 results in loss of ToMV and TMV infectivity in tomato and *Nicotiana benthamiana*. (a) Tomato plants (cv. Moneymaker) homozygous to the *tm-2* or *Tm-2²* allele infected with ToMV, ToMV whose original movement protein was replaced by MP^{ToBRFV}, and ToMV with the C68H mutation in the MP open reading frame. (b) Western blot analysis of ToMV CP in young leaves of *tm-2* and *Tm-2²* plants infected with ToMV expressing the various MPs. Images and leaf samples were taken at 13 days postinoculation (dpi). (c) White light (top) and UV light (bottom) images of *N. benthamiana* plants infected with TMV-GFP infectious clones harbouring MP^{TMV} (left), MP^{ToBRFV} (middle), or MP^{TMV C68H} (right). (d) In vivo imaging-based quantitative analysis of green fluorescent protein (GFP) fluorescence in systemic leaves (fourth leaf from the apex) of plants infected with TMV-GFP harbouring the different movement proteins (MP^{TMV}, MP^{ToBRFV}, or MP^{TMV C68H}). Images were taken at 10 dpi. Different letters indicate significance in Tukey's HSD test ($p < 0.05$, $n \geq 4$).

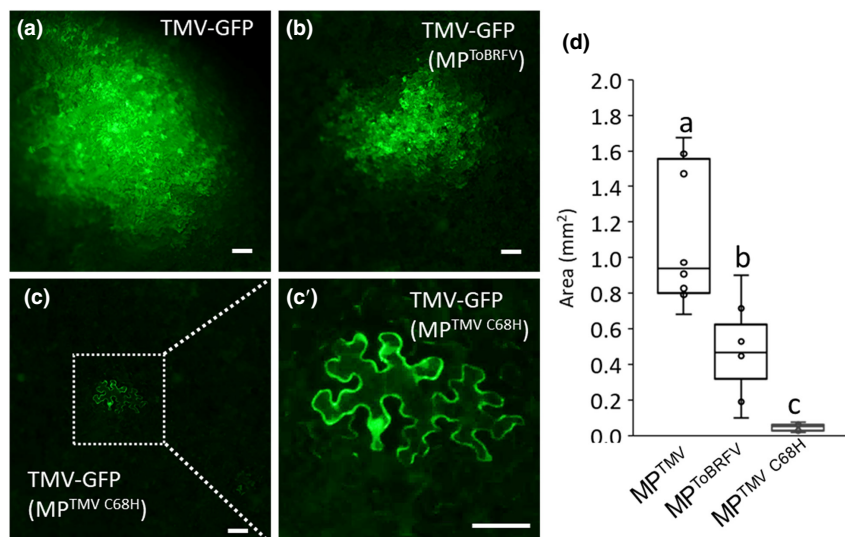


FIGURE 4 Substitution of MP^{TMV} amino acid C68 results in loss of viral cell-to-cell movement. (a–c) Cell-to-cell movement of the TMV-GFP infectious clones harbouring MP^{TMV} (a), MP^{ToBRFV} (b), or MP^{TMV C68H} (c) at 5 days postinoculation. Magnification of the segmented section in the upper panel showing the failure of TMV-GFP MP^{TMV C68H} to move out of the infected cell is shown in (c'). (d) Quantification of infection foci area. Different letters above bars indicate significance in Tukey's HSD test ($p < 0.05$, $n \geq 9$). Scale: 100 μm.

the plasma membrane, as observed by colocalization with the Flot1-RFP plasma membrane marker (Figure 6d,e). It is important to note that the level of PD localization did not correlate with the MP-YFP fluorescence levels at the whole cell (Figure S6), suggesting that the mislocalization of MP^{TMV(C68H)}-YFP was not a result of reduced protein accumulation. These results indicate that C68 is required for the MP^{TMV} intercellular transport function by targeting it to PD.

As shown in Figure 2, C68 is part of an ER interaction motif. Because targeting of MP to PD requires its interaction with the ER network (Wright et al., 2007), we postulated that the C68H mutation may alter MP^{TMV} interaction with the ER. To address this, we used confocal microscopy to image the upper plane of *N. benthamiana* epidermal cells co-expressing ER-mCherry with either MP^{TMV}-YFP or MP^{TMV(C68H)}-YFP (Figure 7). In these regions, MP^{TMV}-YFP

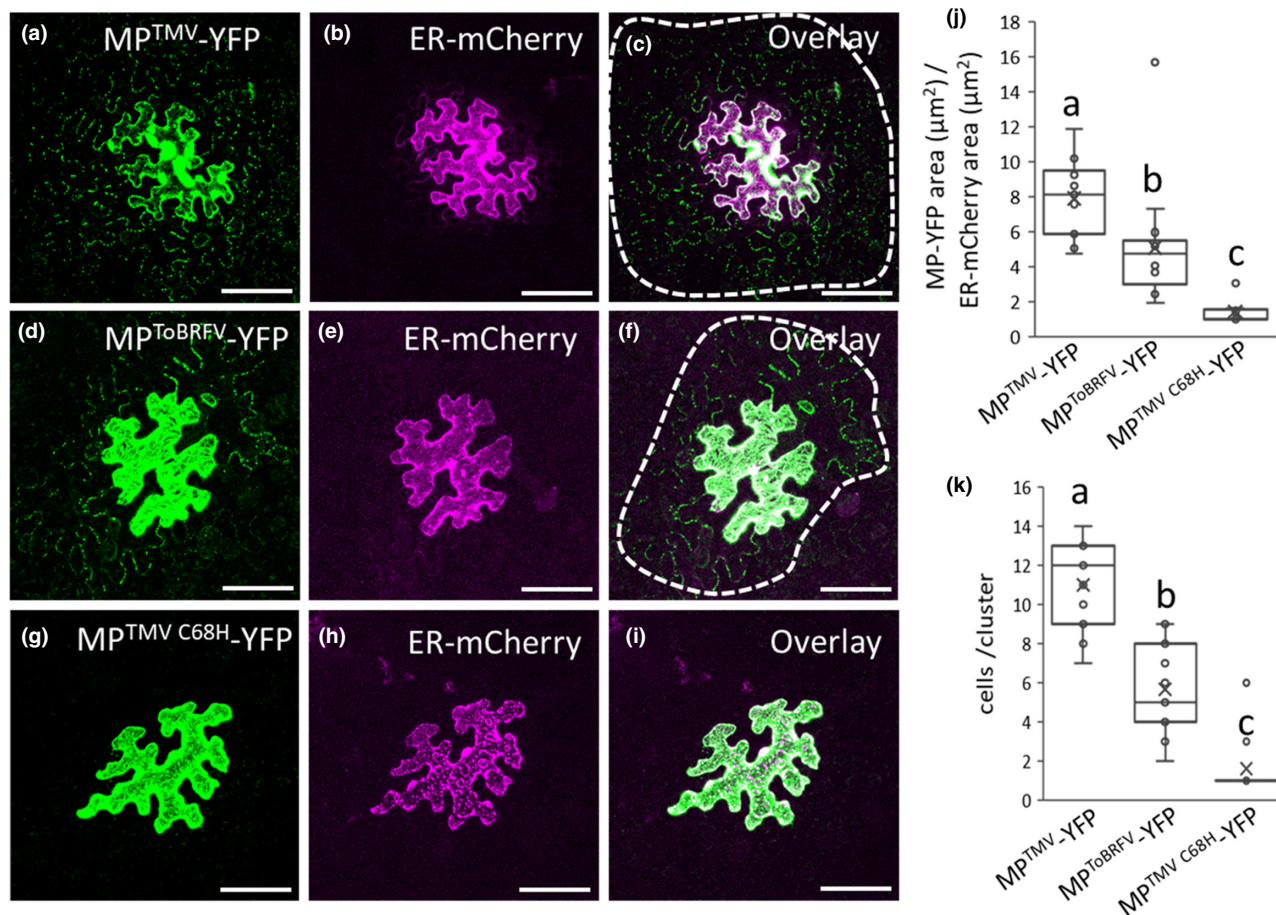


FIGURE 5 C68 is essential for MP^{TMV} intercellular movement. (a–c) Z-stack maximal projection confocal images of a *Nicotiana benthamiana* leaf epidermal cell expressing MP^{TMV}-YFP (a), the nonmobile endoplasmic reticulum (ER)-mCherry marker (b), and their overlay (c). (d–f) Z-stack maximal projection confocal images of epidermal cells expressing MP^{ToBRFV}-YFP (d), ER-mCherry (e), and their overlay (f). (g–i) Z-stack maximal projection confocal images of epidermal cells expressing MP^{TMV C68H}-YFP (g), ER-mCherry (h), and their overlay (i). (j) Quantitative analysis of the ratio between the area of MP^{TMV}-YFP, MP^{ToBRFV}-YFP, and MP^{TMV C68H}-YFP signal and the area of ER-mCherry signal. (k) Quantitative analysis of the number of cells per MP^{TMV}-YFP or MP^{ToBRFV}-YFP and MP^{TMV C68H}-YFP cluster. Different letters indicate significance in Tukey's HSD test ($p < 0.05$, $n \geq 11$). Scale: 100 μm .

formed vesicles that were 76% colocalized with the ER (Figure 7a–c,g). On the other hand, the localization of MP^{TMV(C68H)}-YFP was altered to microdomain-like structures, and the colocalization with the ER was calculated at only 48% (Figure 7b–g). We further used live confocal imaging to assess the ability of the MP to traffic on the ER network. The MP^{TMV}-YFP-associated vesicles were largely mobile, with an average velocity of 1.48 $\mu\text{m}/\text{s}$ (Figure 7h,l and Video S1). In marked contrast, MP^{TMV(C68H)}-YFP bodies were largely immobile (Figure 7h,i and Video S2). These results suggest that C68 is required for MP^{TMV} targeting to PD by regulating its association with the ER.

3 | DISCUSSION

The co-evolution of *R* genes and their effectors (also known as *Avr* factors) is a major driving force in the arms race between plants and pathogens. The durability of *R* genes relies on the importance

and conservation of its targeted effector (Jones & Dangl, 2006). A successful *R* gene will therefore target effector elements essential for pathogen infectivity and/or survival. However, there are only a few known examples for the mechanisms underlying such trade-offs. Previously, we have shown that overcoming *Tm-2*² by MP^{ToBRFV} was associated with an attenuation of viral movement (Hak & Spiegelman, 2021), suggesting that the elements required for evading *Tm-2*² also function in MP intercellular movement. Here we show that among the amino acids required to overcome *Tm-2*² (Yan et al., 2021), H67 localizes to a critical site for MP function, replacing a cysteine (C68) conserved among Solanaceae-infecting tobamoviruses, and placed within a structure conserved among multiple movement proteins. Substitution of MP^{ToBRFV} H67 with cysteine triggered *Tm-2*² resistance, suggesting that the presence of this amino acid in the context of the viral MP activates *Tm-2*². This is consistent with a previous finding that H67C substitution disabled the capacity of ToBRFV to systemically infect plants harbouring *Tm-2*² (Yan et al., 2021). Interestingly, our results show that the same

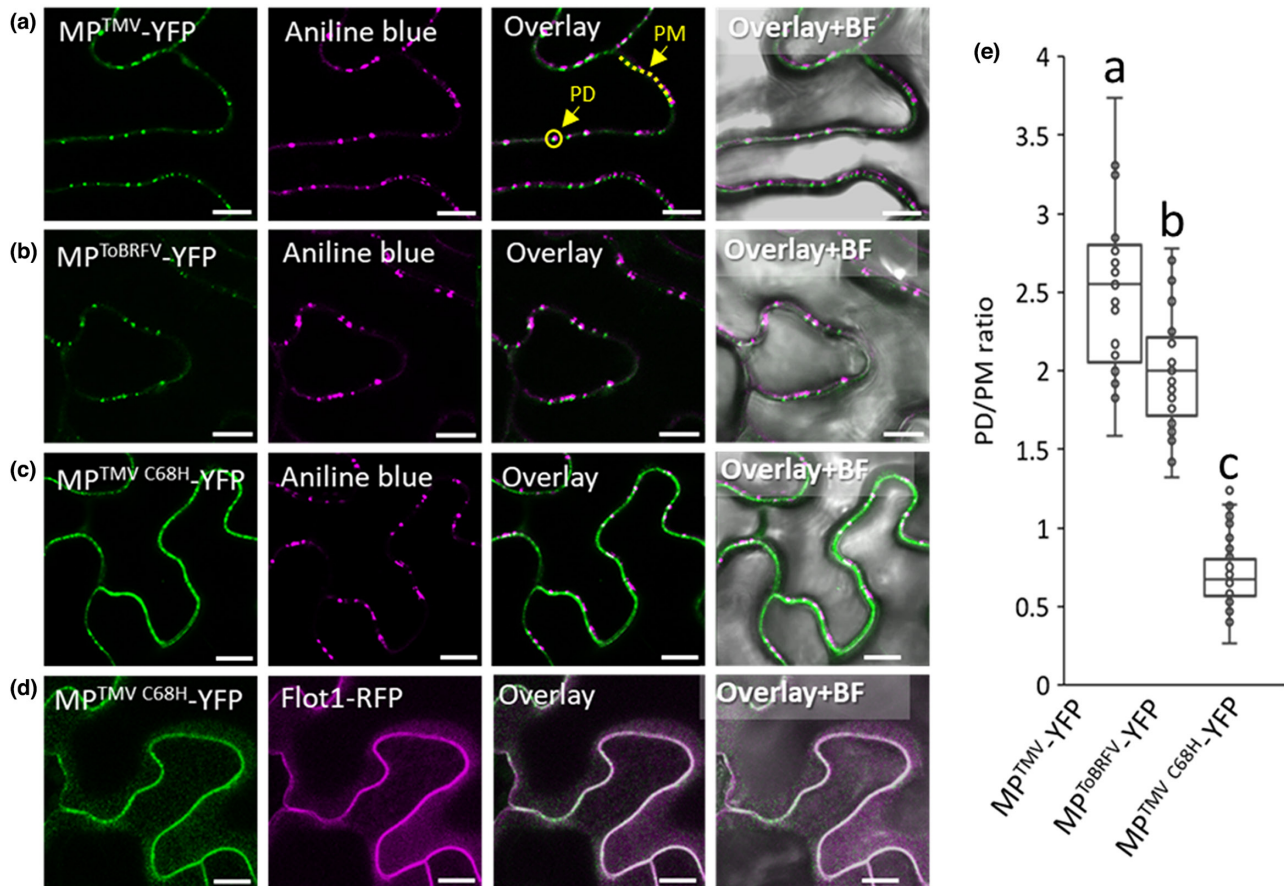


FIGURE 6 C68 is essential for MP^{TMV} plasmodesmatal localization. Localization of MP^{TMV}-YFP (a), MP^{ToBRFV}-YFP (b), and MP^{TMV C68H}-YFP (c) proteins (green) to plasmodesmata (PD) (purple). Plasmodesmata were labelled using aniline blue callose staining. Note that the MP^{TMV C68H}-YFP (c) fails to specifically be targeted to PD. (c) Quantitative analysis of the accumulation of the various MP-YFP proteins in PD. The calculation was based on the ratio between MP-YFP signal in PD and the average fluorescent signal in the plasma membrane (PM). Different letters indicate significance in Tukey's HSD test ($p < 0.05$, $n \geq 25$). Scale: 10 μm .

cysteine is essential for the function of ToMV and TMV by enabling MP subcellular targeting to PD via the ER.

The ER plays a major role in TMV intercellular transport (Pitzalis et al., 2018). Initially, TMV replication complexes are associated with the ER. Then, MP^{TMV}-associated complexes detach and move along the ER membrane to be targeted to PD (Guenoune-Gelbart et al., 2008; Sambade et al., 2008; Wright et al., 2007). The interaction of MP^{TMV} is mediated by two hydrophobic regions, which associate, but do not integrate into the ER membrane. These regions span amino acids 61–80 and 148–167. Although sequentially distant, our AlphaFold-based homology model predicted these two sections to be topologically interacting and take part in a putative jelly-roll fold common to various MPs (Figure 2b-d). These results suggest that Tm-2² targets the viral MP in an element crucial for its function.

There are only few examples in which resistance-breaking mutations cause penalties in viral infectivity or competition (García-Arenal & Fraile, 2013). Mutations in the potato virus Y Nla protein that enable it to overcome the Ry-mediated resistance also caused loss of its protease activity (Mestre et al., 2003). Mutations in turnip mosaic virus that overcome *TuRB01* and *TuRB04* resistances in *Brassica napus* impaired the virus's ability to compete with a

nonresistance-breaking viral strain on a susceptible host (Jenner et al., 2002). *Tm-1* resistance-breaking mutations in the ToMV replicase delay viral replication in tobacco protoplasts (Ishibashi et al., 2012). Mutations in pepper mild mottle virus CP that break L-mediated resistance in pepper were associated with high fitness penalties (Fraile et al., 2011). However, recently it was shown that the effect of resistance-breaking mutations is more complex and depends on the specific mutation, the host genotype, and the infecting isolate (Moreno-Pérez et al., 2016).

Hall (1980) suggested that the durability of *Tm-2*²-mediated resistance against TMV and ToMV was a result of the reduced capacity of these viruses to evolve to overcome *Tm-2*², and predicted that this mutation would probably alter fundamental viral characteristics. Our finding that overcoming *Tm-2*² requires the substitution of C68, which is essential for viral movement, supports this hypothesis. In light of these findings, how was ToBRFV able to overcome this resistance, whereas TMV and ToMV failed to do so? Previous lineage analysis predicted that ToBRFV probably evolved on an unknown host other than tomato, and invaded tomato due to a host-shifting event (Maayan et al., 2018). This allowed MP^{ToBRFV} to diverge from MP^{TMV} and MP^{ToMV} in multiple elements, including C68/H67, while

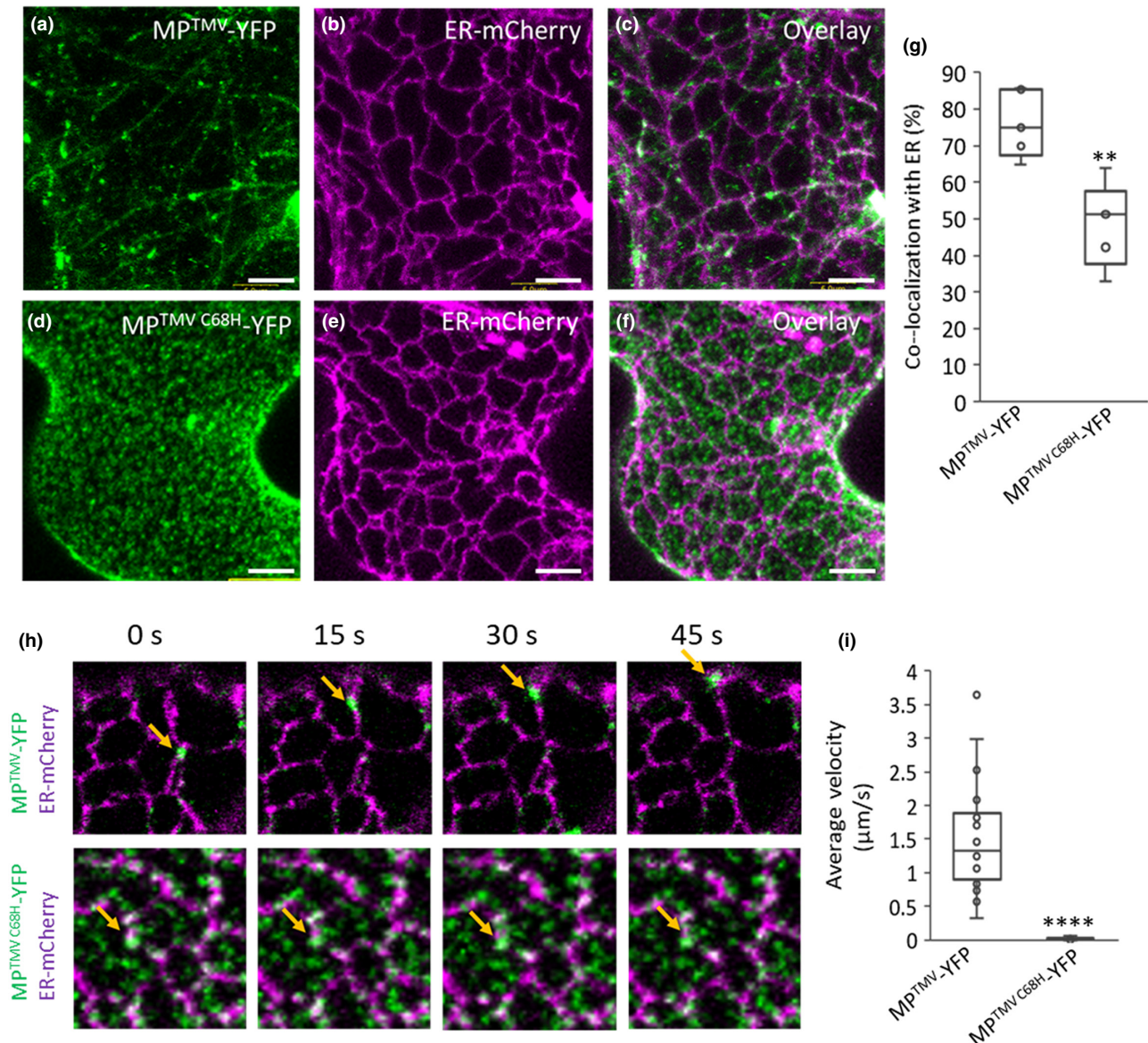


FIGURE 7 C68 is required for MP^{TMV} interaction with the endoplasmic reticulum (ER) and intracellular movement. Surface imaging of upper *Nicotiana benthamiana* leaf epidermal cell planes. (a–c) Expression of MP^{TMV}-YFP (a), ER-mCherry (b), and an overlay of both proteins (c). (d–f) expression of MP^{TMV C68H}-YFP (d), ER-mCherry (e), and an overlay of both proteins (f). (g) Quantitative analysis of MP^{TMV}-YFP and MP^{TMV C68H}-YFP colocalization with ER-mCherry. (h) Dynamics of MP^{TMV}-YFP (top) and MP^{TMV C68H}-YFP (bottom) on the ER network. Note that while MP^{TMV}-YFP are mobile on the ER, MP^{TMV C68H}-YFP are immobile (yellow arrow). (i) Quantification of MP^{TMV}-YFP and MP^{TMV C68H}-YFP vesicle velocity. Scale = 5 μm (** $p < 0.01$, **** $p < 0.0001$ in Student's t test, $n \geq 24$).

sustaining viral movement. On the other hand, in TMV and ToMV, loss of C68 would require additional compensatory mutations for MP to retain functionality. The requirement of multiple mutations to overcome $Tm-2^2$ combined with high levels of fitness penalties would be highly unlikely or rare and uncompetitive.

Collectively, we find that the conversion of cysteine at position 67 (H67) in MP^{ToBRFV} is crucial for evading $Tm-2^2$ resistance. However, in MP^{TMV}, substitution of cysteine in the corresponding position (C68) results in the abolition of cell-to-cell movement. We conclude that this strong trade-off between viral movement and breaking host resistance could be one of the primary reasons for the high durability of $Tm-2^2$ against TMV and ToMV for over 60 years.

4 | EXPERIMENTAL PROCEDURES

4.1 | Plant materials

Tomato (*Solanum lycopersicum*) seeds (cv. Moneymaker) homozygous for the $tm-2$ allele (LA2706) or the $Tm-2^2$ allele (LA3310) were obtained from the Tomato Genome Research Center, University of California, Davis. *N. benthamiana* and tomato plants were grown in soil in a light- and temperature-controlled chamber at 25°C in a 16-h photoperiod. Five-week-old *N. benthamiana* plants were used for agroinfiltration and 3-week-old tomato plants were used for mechanical inoculation of ToMV.

4.2 | Plasmid construction

Plasmids p35S:TM-2², p35S:MP^{TMV}, p35S:MP^{ToBRFV}, p35S:MP^{TMV}-YFP+ER-mCherry and p35S:MP^{ToBRFV}-YFP+ER-mCherry were assembled by Golden Gate cloning using the MoClo tool kit for plants (Addgene) (Weber et al., 2011) as described by Hak and Spiegelman (2021). Generation of the vectors TMV-GFP^{MP-ToBRFV} and ToMV^{MP-ToBRFV}, based on the pJL24 (Lindbo, 2007) and pTLW3 (Hamamoto et al., 1993), were described previously (Hak & Spiegelman, 2021). Hybrid movement proteins were generated using fusion PCR. All the constructs that contain point mutations were made using site-directed mutagenesis (Ho et al., 1989) and confirmed by sequencing.

4.3 | Transient expression and agroinfiltration

Agrobacterium tumefaciens EHA105 harbouring a binary vector was grown overnight at 28°C. Cell cultures were resuspended in 2-morpholinoethane sulfonic acid (MES) buffer (10mM MgCl₂, 10mM MES, 150µM acetosyringone, pH 5.6) to OD₆₀₀ = 0.5. For MP-YFP and TMV-GFP cell-to-cell movement assays, OD₆₀₀ = 0.0001 and OD₆₀₀ = 5e⁻⁶ were used, respectively. *Agrobacterium* solutions were infiltrated using a needleless syringe into the abaxial side of the fourth or fifth leaf of *N. benthamiana* plants.

4.4 | Electrolyte leakage assay

p35S:MP constructs were agroinfiltrated into *N. benthamiana* leaves ($n = 4$) at OD₆₀₀ = 0.25 at a 1:1 ratio with either p35S:TM-2² or an empty vector. Twenty-seven hours after agroinfiltration, four leaf discs (1 cm diameter) were cut from each leaf and washed for 10–30min in distilled water. The leaf discs were then carefully transferred into a tube containing 4 mL of distilled water and placed on a low speed orbital shaker. Electric conductivity was measured after 6 h using a benchtop conductivity meter. Each experiment was repeated at least three times.

4.5 | TMV-GFP infection and quantification

For systemic infection experiments, *A. tumefaciens* harbouring TMV-GFP or TMV-GFP^{MP-ToBRFV} vectors at OD₆₀₀ = 0.25 were infiltrated at a 1:1 ratio with the silencing suppressor p19 into the fourth leaf of 4-week-old *N. benthamiana* plants. GFP fluorescence was monitored 6 days postinfiltration. Images were acquired and analysed using an IVIS Lumina LT (PerkinElmer) equipped with a XFOV-24 lens and Living Image v. 4.3.1 software (PerkinElmer) set (excitation/emission: 420nm/520nm). The optical luminescent image data were displayed in pseudocolour that represents intensity in terms of radiance (photons per second per square centimetre per steradian) and were calculated as average radiance per

leaf. For cell-to-cell movement of TMV-GFP, imaging of GFP was obtained and analysed at 5 days postinoculation (dpi) using a Nikon SMZ-25 stereomicroscope equipped with a Nikon-D2 camera and NIS Elements v. 5.11 software. The number of plants for each experiment was $n = 4$ and experiments were repeated at least three times.

4.6 | In vitro transcription and infection of ToMV

Two microlitres of ToMV pTLW3 plasmid, ToMV^{MP-ToBRFV}, or ToMV^{MP-TMV(C68H)} were linearized with *Sma*I and were prepared by a gel extraction kit (Zymo Research). In vitro transcription was performed using the mMESAGE mMACHINE T7 kit (Invitrogen by Thermo Fisher Scientific). Two drops of 2.5 µL of transcript were used to mechanically inoculate *N. benthamiana* plants dusted with carborundum powder prior to inoculation. Leaves of infected plants were collected 5–7 dpi to serve as inoculum for 3-week-old tomato plants.

4.7 | Detection of ToMV by immunoblotting

For detection of the systemic spread of the virus in tomato, the first young leaf (10–30mm) and apex were collected and ground, while frozen, in a microcentrifuge tube. Laemmli buffer (40µL of 3x) (100mM Tris, 2% SDS, 20% glycerol, 4% β-mercaptoethanol, pH 6.8) was added and mixed into the sample, followed by centrifugation for 10 min and boiling of the supernatant for 5 min. Samples were run on 12% SDS-polyacrylamide gels, transferred to nitrocellulose membranes (Protran), and were blocked with 3% skimmed milk in Tris-buffered saline with Tween. Coat protein (CP) of the virus was detected by rabbit anti-tobamovirus CP (1:20,000; courtesy of A. Dombrovsky) and anti-rabbit horseradish peroxidase (1:20,000; Jackson Immunoresearch). Chemiluminescence was observed using Elistar Supernova as substrate (Cyanagen), and images of protein bands were acquired using the Alliance UVITEC software.

4.8 | Cell-to-cell movement analysis of MP-YFP

Experiments were performed as previously described (Hak & Spiegelman, 2021). Constructs expressing both MP-YFP and ER-mCherry were agroinfiltrated into *N. benthamiana* and visualized 36 h later. For confocal imaging, we used an Olympus IX 81 inverted laser scanning confocal microscope (Fluoview 500) equipped with an OBIS 488 and 561 nm laser lines, and a 60x1.0 NA PlanApo water immersion objective. YFP and mCherry were excited at 488 and 561 nm and were imaged using BA505-525 nm and BA575-620 nm emission filters, respectively. The number of YFP-fluorescent cells surrounding the original cell of expression was quantified to determine the level of movement for each MP.

4.9 | Subcellular localization of MP-YFP

For ER localization, double expression plasmids harbouring MP-YFP and ER-mCherry were used (Hak & Spiegelman, 2021). For PM localization, MP-YFP was co-expressed with Flotilin1 fused to RFP under the 35S promoter (Flot1-RFP) (Pizarro et al., 2019). For plasmodesmatal localization, aniline blue solution (0.1% in water) was infiltrated into the abaxial side of the leaf and 10 min later imaged. Images were taken using an Olympus IX 81 inverted laser scanning confocal microscope (Fluoview 500). Excitation of aniline blue at 405 nm was done using a BA430–460 filter with an UPlanSApo 60×1.35 oil objective, 8/0.17 FN26.5. Quantification of MP-YFP accumulation intensity in PD, PM, and ER was performed using the ImageJ software (<https://imagej.nih.gov/ij/>) by measuring the YFP signal intensity colocalized with each of the markers.

4.10 | Multiple sequence alignment

Sequence alignment of the Solanaceae-infecting tobamoviruses MPs pepper mild mottle virus (NP_619742.1), bell pepper mottle virus (YP_001333652.1), Rehmannia mosaic virus (YP_001041891.1), TMV (NP_597748.1), ToBRFV (YP_009182170.1), ToMV (NP_078448.1), tomato mottle mosaic virus (YP_008492930.1), Obuda pepper virus (NP_620843.1), paprika mild mottle virus (NP_671720.1), Brugmansia mild mottle virus (YP_001974325.1), and tobacco mild green mosaic virus (sp|P18338|) was performed using Clustal Omega (<https://www.ebi.ac.uk/Tools/msa/clustalo/0>).

4.11 | Protein structure prediction using AlphaFold2

The 3D structures of MP^{TMV} (NP_597748.1), MP^{ToBRFV} (YP_009182170.1), MP^{CaMV} (NP_056724.1), MP^{CMV} (NP_040776.1), MP^{TBSV} (NP_062900.1), and MP^{TSWV} (AEK06236.1) were predicted using the artificial Intelligence-based AlphaFold2 through the AlphaFold Colab notebook platform (Jumper et al., 2021). For the structural comparisons, we used only the predicted model with the highest confidence score computed by AlphaFold for each protein. The PyMOL Molecular Graphics System (v. 2.4, Schrödinger) was used to examine the structural models and generate images.

ACKNOWLEDGEMENTS

We thank M. Heinlein (French National Centre for Scientific Research), B. Falk (University of California Davis), and M. Ishikawa (Japanese National Agriculture and Food Research Organization) for providing the TMV-GFP and ToMV infectious clones. We thank A. Dombrovsky for anti-tobamovirus CP antibody and I. Levin (Agriculture Research Organization, Israel) for the tomato (cv. Moneymaker) lines used. We thank V. Gaba (Agriculture Research Organization, Israel) for critical reading of this manuscript.

FUNDING INFORMATION

This study was funded by the Israeli Ministry of Agriculture and Rural Development research grant 20-02-0130 and the US-Israel Agricultural Research and Development Fund (BARD) research grant IS-5386-21R.

DATA AVAILABILITY STATEMENT

The data that support the findings of this study are available from the corresponding author upon reasonable request.

ORCID

Savithramma P. Dinesh-Kumar  <https://orcid.org/0000-0001-5738-316X>

Ziv Spiegelman  <https://orcid.org/0000-0003-4876-5072>

REFERENCES

- Adachi, H., Derevnina, L. & Kamoun, S. (2019) NLR singletons, pairs, and networks: evolution, assembly, and regulation of the intracellular immunoreceptor circuitry of plants. *Current Opinion in Plant Biology*, 50, 121–131.
- Bi, G., Su, M., Li, N., Liang, Y., Dang, S., Xu, J. et al. (2021) The ZAR1 resistosome is a calcium-permeable channel triggering plant immune signaling. *Cell*, 184, 3528–3541.
- Broadbent, L. (1976) Epidemiology and control of tomato mosaic virus. *Annual Review of Phytopathology*, 14, 75–96.
- Chen, T., Liu, D., Niu, X., Wang, J., Qian, L., Han, L. et al. (2017) Antiviral resistance protein Tm-2² functions on the plasma membrane. *Plant Physiology*, 173, 2399–2410.
- Citovsky, V., Wong, M.L., Shaw, A.L., Venkataram Prasad, B.v. & Zambryskii, P. (1992) Visualization and characterization of tobacco mosaic virus movement protein binding to single-stranded nucleic acids. *The Plant Cell*, 4, 397–438.
- Fraile, A., Pagan, I., Anastasio, G., Saez, E. & Garcia-Arenal, F. (2011). Rapid genetic diversification and high fitness penalties associated with pathogenicity evolution in a plant virus. *Molecular Biology and Evolution*, 28, 1425–1437.
- García-Arenal, F. & Fraile, A. (2013) Trade-offs in host range evolution of plant viruses. *Plant Pathology*, 62, 2–9.
- Goelet, P., Lomonosoff, G.P., Butler, P.J.G., Akam, M.E., Gait, M.J. & Karn, J. (1982) Nucleotide sequence of tobacco mosaic virus RNA. *Proceedings of the National Academy of Sciences of the United States of America*, 79, 5818–5822.
- Guenoune-Gelbart, D., Elbaum, M., Sagi, G., Levy, A. & Epel, B.L. (2008) Tobacco mosaic virus (TMV) replicase and movement protein function synergistically in facilitating TMV spread by lateral diffusion in the plasmodesmal desmotubule of *Nicotiana benthamiana*. *Molecular Plant-Microbe Interactions*, 21, 335–345.
- Hak, H. & Spiegelman, Z. (2021) The tomato brown rugose fruit virus movement protein overcomes Tm-2² resistance in tomato while attenuating viral transport. *Molecular Plant-Microbe Interactions*, 9, 1024–1032.
- Hall, T.J. (1980) Resistance at the Tm-2 locus in the tomato to tomato mosaic virus. *Euphytica*, 29, 189–197.
- Hamamoto, H., Sugiyama, Y., Nakagawa, N., Hashida, E., Matsunaga, Y., Takemoto, S. et al. (1993) A new tobacco mosaic virus vector and its use for the systemic production of angiotensin-1-converting enzyme inhibitor in transgenic tobacco and tomato. *Biotechnology*, 11, 930–932.
- Ho, S.N., Hunt, H.D., Horton, R.M., Pullen, J.K. & Pease, L.R. (1989) Site-directed mutagenesis by overlap extension using the polymerase chain reaction. *Gene*, 77, 51–59.

- Ishibashi, K., Mawatari, N., Miyashita, S., Kishino, H., Meshi, T. & Ishikawa, M. (2012) Coevolution and hierarchical interactions of tomato mosaic virus and the resistance gene *Tm-1*. *PLoS Pathogens*, 8, e1002975.
- Jenner, C.E., Wang, X., Ponz, F. & Walsh, J.A. (2002) A fitness cost for turnip mosaic virus to overcome host resistance. *Virus Research*, 86, 1–6.
- Jones, J.D.G. & Dangl, J.L. (2006) The plant immune system. *Nature*, 444, 323–329.
- Jumper, J., Evans, R., Pritzel, A., Green, T., Figurnov, M., Ronneberger, O. et al. (2021) Highly accurate protein structure prediction with AlphaFold. *Nature*, 596, 583–589.
- Krupovic, M., Makarova, K.S. & Koonin, E.V. (2022) Cellular homologs of the double jelly-roll major capsid proteins clarify the origins of an ancient virus kingdom. *Proceedings of the National Academy of Sciences of the United States of America*, 119, e2120620119.
- Lindbo, J.A. (2007) High-efficiency protein expression in plants from agroinfection-compatible tobacco mosaic virus expression vectors. *BMC Biotechnology*, 7, 52.
- Luria, N., Smith, E., Reingold, V., Bekelman, I., Lapidot, M., Levin, I. et al. (2017) A new Israeli *Tobamovirus* isolate infects tomato plants harboring *Tm-2²* resistance genes. *PLoS One*, 12, e0170429.
- Maayan, Y., Pandaranayaka, E.P.J., Srivastava, D.A., Lapidot, M., Levin, I., Dombrovsky, A. et al. (2018) Using genomic analysis to identify tomato *Tm-2* resistance-breaking mutations and their underlying evolutionary path in a new and emerging tobamovirus. *Archives of Virology*, 163, 1863–1875.
- Martin, R., Qi, T., Zhang, H., Liu, F., King, M., Toth, C. et al. (2020) Structure of the activated ROQ1 resistosome directly recognizing the pathogen effector XopQ. *Science*, 370, eabd9993.
- Meier, N., Hatch, C., Nagalakshmi, U. & Dinesh-Kumar, S.P. (2019) Perspectives on intracellular perception of plant viruses. *Molecular Plant Pathology*, 20, 1185–1190.
- Mestre, P., Brigneti, G., Durrant, M.C. & Baulcombe, D.C. (2003) Potato virus Y Nla protease activity is not sufficient for elicitation of R_y-mediated disease resistance in potato. *The Plant Journal*, 36, 755–761.
- Moreno-Pérez, M.G., García-Luque, I., Fraile, A. & García-Arenal, F. (2016) Mutations that determine resistance breaking in a plant RNA virus have pleiotropic effects on its fitness that depend on the host environment and on the type, single or mixed, of infection. *Journal of Virology*, 90, 9128–9137.
- Navarro, J.A., Sanchez-Navarro, J.A. & Pallas, V. (2019) Key checkpoints in the movement of plant viruses through the host. *Advances in Virus Research*, 104, 1–64.
- Peiro, A., Martinez-Gil, L., Tamborero, S., Pallas, V., Sanchez-Navarro, J.A., Mingarro, I. et al. (2014) The tobacco mosaic virus movement protein associates with but does not integrate into biological membranes. *Journal of Virology*, 88, 3016–3026.
- Pitzalis, N., Heinlein, M., Pietro, G. & Sansebastiano, D. (2018) The roles of membranes and associated cytoskeleton in plant virus replication and cell-to-cell movement. *Journal of Experimental Botany*, 69, 117–132.
- Pizarro, L., Leibman-Markus, M., Schuster, S., Bar, M. & Avni, A. (2019) Tomato dynamin related protein 2A associates with LeEIX2 and enhances PRR mediated defense by modulating receptor trafficking. *Frontiers in Plant Science*, 10, 936.
- Reagan, B.C. & Burch-Smith, T.M. (2020) Viruses reveal the secrets of plasmodesmal cell biology. *Molecular Plant-Microbe Interactions*, 33, 26–39.
- Sambade, A., Brandner, K., Hofmann, C., Seemanpillai, M., Mutterer, J. & Heinlein, M. (2008) Transport of TMV movement protein particles associated with the targeting of RNA to plasmodesmata. *Traffic*, 9, 2073–2088.
- Wang, J., Hu, M., Wang, J., Qi, J., Han, Z., Wang, G. et al. (2019) Reconstitution and structure of a plant NLR resistosome conferring immunity. *Science*, 364, eaav5870.
- Wang, J., Chen, T., Han, M., Qian, L., Li, J., Wu, M. et al. (2020) Plant NLR immune receptor *Tm-2²* activation requires NB-ARC domain-mediated self-association of CC domain. *PLoS Pathogens*, 16, e1008475.
- Weber, H., Schultze, S. & Pfitzner, A.J. (1993) Two amino acid substitutions in the tomato mosaic virus 30-kilodalton movement protein confer the ability to overcome the *Tm-2²* resistance gene in the tomato. *Journal of Virology*, 67, 6432–6438.
- Weber, E., Gruetzner, R., Werner, S., Engler, C. & Marillonnet, S. (2011) Assembly of designer TAL effectors by Golden Gate cloning. *PLoS One*, 6, e19722.
- Wright, K.M., Wood, N.T., Roberts, A.G., Chapman, S., Boevink, P., MacKenzie, K.M. et al. (2007) Targeting of TMV movement protein to plasmodesmata requires the Actin/ER network; evidence from FRAP. *Traffic*, 8, 21–31.
- Yan, Z.Y., Ma, H.Y., Wang, L., Tettey, C., Zhao, M.S., Geng, C. et al. (2021) Identification of genetic determinants of tomato brown rugose fruit virus that enable infection of plants harbouring the *Tm-2²* resistance gene. *Molecular Plant Pathology*, 22, 1347–1357.
- Zhang, S., Griffiths, J.S., Marchand, G., Bernards, M.A. & Wang, A. (2022) *Tomato brown rugose fruit virus*: an emerging and rapidly spreading plant RNA virus that threatens tomato production worldwide. *Molecular Plant Pathology*, 23, 1262–1277.

SUPPORTING INFORMATION

Additional supporting information can be found online in the Supporting Information section at the end of this article.

How to cite this article: Hak, H., Raanan, H., Schwarz, S., Sherman, Y., Dinesh-Kumar, S.P. & Spiegelman, Z. (2023) Activation of *Tm-2²* resistance is mediated by a conserved cysteine essential for tobacco mosaic virus movement. *Molecular Plant Pathology*, 24, 838–848. Available from: <https://doi.org/10.1111/mpp.13318>